Non-conventional charge transport in organic semiconductors: magnetoresistance and thermoelectricity

FENWICK, OJ; Orgiu, E

Journal Name

ARTICLE

Beyond charge transport in organic semiconductors: Magnetoresistance and thermoelectricity.

Oliver Fenwick*[a] and Emanuele Orgiu *[b]

Received 00th January 20xx,
Accepted 00th January 20xx

DOI: 10.1039/x0xx00000x

www.rsc.org/

High mobility charge transport in various organic semiconductors is now well documented and well understood. As a result, research is now focussing on more exotic transport properties driving a new generation of organic electronic devices. This mini-review will focus on the two most prominent of these, magnetoresistance and thermoelectricity. Each requires additional properties of materials beyond their ability to transport charge, namely a large resistive response to a magnetic field, or in the case of thermoelectrics a large Seebeck coefficient combined with low thermal conductivity. This mini-review will explore the current state of the art in organic materials for these applications and will discuss current ideas on the molecular and structural origins of their properties with an outlook on future directions for molecular design.

1. Organic Magnetoresistance (OMAR) effects

1.1 Introduction to OMAR

In the past decade organic electronics crossed the path of the field of spintronics with increasing attention being focussed on spin physics and magnetic field effects in organic π-conjugated systems.[4] More recently, large magnetic field effects were measured at room temperature in organic semiconductors with *non*-magnetic electrodes i.e. without any spin-injection into the active layer. These effects are known collectively as magnetoelectroluminescence and the magnetoresistance[5-8], with the latter sometimes referred to as organic magnetoresistance (OMAR) and defined as

$$\frac{\Delta R}{R(0)} \equiv \frac{R(B) - R(0)}{R(0)} \quad (1)$$

(where R is the device resistance measured with no applied magnetic field, R(0), and with an applied magnetic field, R(B)). In some organic materials, OMAR reaches up to 10% at room temperature for very low magnetic fields, e.g. B = 10 mT.[10] The magnetoresistance effect is therefore amongst the largest of any *non*magnetic bulk material. OMAR immediately garnered much attention from the scientific community[6-8, 11-30] because of its huge potential that could be translated into intriguing technological applications. OMAR devices do not require ferromagnetic electrodes which offers a much higher degree of freedom in the material choice not achievable for other magnetoresistive or conventional organic-based spintronic devices. Just like organic electronic devices, they can be fabricated at low cost on flexible substrates and, in principle, they can also be transparent. Devices using OMAR are therefore promising for applications where large numbers of magnetoresistive devices are needed, e.g. magnetic random-access-memory (MRAM) but also in touch screens based on OLED technology, in which the spatial coordinates of a magnetic stylus could be sensed.

The main mechanism proposed for explaining the OMAR effect is based on bipolaron formation[7, 19, 26]. Charge carrier interactions in organic semiconductors are mediated by vibrational fields, and the nature of such interactions is attractive even in charge pairs of the same sign, i.e. electron-electron or hole-hole. A charge along with its vibrational field forms a so-called "*polaron*". Because of the large electron-phonon coupling, the polaron conduction in disordered materials occurs mostly via hopping between localized sites. As anticipated, it is possible, in principle, that two positively (hole) or negatively (electron) charged polarons share the same site. Normally, the Coulomb repulsion, governed by the potential energy *U*, should oppose the formation of *bipolaron*s, i.e. two (small) polarons localized either at the same lattice site or at two different but neighbouring lattice sites. Whether or not the two holes (or electrons) can remain at the same site, is determined by the interplay between the effective potential, which arises if both the Coulomb repulsion, and the electron (hole)-phonon or polaron interaction. If the polaron interaction dominates the Coulomb repulsion, the two carriers can occupy the same site. The double occupancy of a lattice site leads to the formation of a bipolaron localized on such site. In addition, whether or not a bipolaron will be formed depends on the spin configuration of the each polaron: when two polarons meet, they possess a randomly oriented spin. A bipolaron can only form in the singlet (ground) state because of on-site exchange effects[31] and a triplet state cannot be formed. When no external magnetic field (B_{ext}) is applied (or when B_{ext} is small compared to the hyperfine field, B_{hf}), the spin of each polaron sitting on a hydrocarbon molecule

[a] School of Engineering and Materials Science, Queen Mary, University of London Mile End Road, London E1 4NS, United Kingdom.
[b] Institut de Science et d'Ingénierie Supramoléculaires (I.S.I.S.), Université de Strasbourg 8, allée Gaspard Monge,F - 67000 Strasbourg, France.

† Footnotes relating to the title and/or authors should appear here.
Electronic Supplementary Information (ESI) available: [details of any supplementary information available should be included here]. See DOI: 10.1039/x0xx00000x

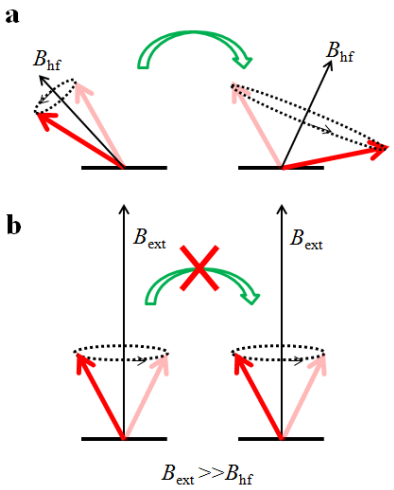

Figure 1: (**a**) No external magnetic field applied allows spin-mixing between two polarons thanks to spin precession; (**b**) When an external magnetic field $B_{ext} >> B_{hf}$ is applied, they both precess about B_{ext} which prevents the formation of the bipolaron and of electrical conduction across that molecule.

precesses about the (random) local magnetic field produced by the hydrogen nuclei, called the hyperfine field (B_{hf}). The random orientation of the B_{hf} associated with each polaron allows a transition to a spin-singlet bipolaron. Consider a pair of polarons, $\mathbf{p}_1$ and $\mathbf{p}_2$, possessing either (i) parallel and antiparallel initial spin (with respect to the local field) or (ii) both parallel initial spin states. In the absence of an external magnetic field, both initial spin states (i) and (ii) can lead to the formation of a spin-singlet bipolaron. This process is called *spin-mixing* and ensures that even a polaron pair that could potentially acquire a triplet character (therefore not forming a bipolaron) can still mix with a singlet character therefore allowing bipolaron formation (Figure 1a). However, when an external magnetic field is applied ($B_{ext} >> B_{hf}$) the spins of the two polarons on different sites can only precess about B_{ext}, which will force the spins of $\mathbf{p}_1$ and $\mathbf{p}_2$ to be parallel. Hence, if $\mathbf{p}_1$ and $\mathbf{p}_2$ were in initial state (ii) a bipolaron could not be formed (Figure 1b). The latter case describes a phenomenon of spin blockade, which makes that specific site no longer available for charge carriers, which will have to take another transport path. Spin blockade over a number of (molecular) sites will generate a decrease in the measured current which is associated to an increase in resistance upon the application of an external magnetic field larger than the hyperfine field. This is magnetoresistance with *positive* sign. In general, the sign is not always positive and it has been found to change as a function of voltage and temperature[5, 12, 14, 20]. The sign change in vertical devices with electroluminescent active layers has been ascribed to a different ratio between majority and minority charge carriers induced by the magnetic field which can cause a decrease (positive magnetoresistance) or an increase (negative magnetoresistance) in device current upon application of B_{ext}.

1.2. Molecular Approaches to engineering OMAR

As introduced previously, the main mechanism proposed for explaining the OMMR effect relies on the fact that the bipolaron formation is magnetic field dependent[7, 19, 26]. In the absence of an external magnetic field, the (hole) polaron formation rate follows the general trend[32, 33]:

$$\frac{dN_h(t)}{dt} = -kN_h(t)^2 + cN_{BP}(t) \qquad (2)$$

where N_h and N_{BP} are the polaron and bipolaron concentrations and k and c are rate constants. Clearly, this relation can be extended to the symmetric case, where electrons are the majority charge carriers.

In a three-terminal device $N_h = C_{ins}\frac{|V_{GS} - V_{TH}|}{t}$ where C_{ins} is the gate dielectric capacitance, t is the thickness of the conductive channel (1-3 nm) and V_{GS}-V_{TH} is the difference between gate-source and threshold voltage respectively. This simple expression reveals that the bipolaron concentration depends on the number of majority carriers involved in the transport which is set by the gate voltage (at a given drain-source voltage which ensures longitudinal electric field). We stress that the use of a three-terminal transistor device for testing bipolaron formation is key as it can induce a high and controllable charge carrier density within the semiconducting film. This allows one to monitor the formation rate of the bipolarons by varying the hole (electron) density. Street et *al.*[33] found that a polyfuorene derivative, F8T2, and regioregular polythiophene both follow the proposed law (equation 2), but their propensity to form bipolarons, expressed by c, differed. This was ascribed to a different bipolaron binding energy and highlights the *strong dependence of bipolaron formation on the specific material*. This picture gets even clearer if one thinks of bipolarons as negative correlation states that should be stabilized through a relaxation of the polymer backbone as a consequence of the formation of a "two-polaron" bound state. The local polymer structure is strongly correlated to the relaxation energy which, again, points towards a dependence of the bipolaron formation on the material and its structural order. Generally speaking, organic polymer semiconductors are polycrystalline and disordered materials and, as a consequence, the degree of order of the film will dictate the local bipolaron concentration within the film as well as the physical location where the bipolaron formation can occur. Further investigations were carried out by the Vardeny group[34] who observed polaron states with different energy in polythiophenes which were ascribed to the presence of an ordered and a disordered phase, respectively. Bipolaron formation is certainly favoured at specific sites within the film. Most likely, bipolarons are formed not in the crystalline portions of the film but rather at the grain boundaries or at the dielectric interface.

Another important observation on how to design polymers which feature high OMAR is given by Kersten et al.[22] In this work, the role of energetic disorder, (intrinsic) dopant strength and interchain hopping is discussed for polymers. The first two are not found to significantly influence the OMAR whilst controlling *inter-* and *intra-*chain transport plays a key role. In particular, precise molecular design rules are provided such as: (i) reducing the coupling between each monomer unit in order to reduce the hopping vs. hyperfine

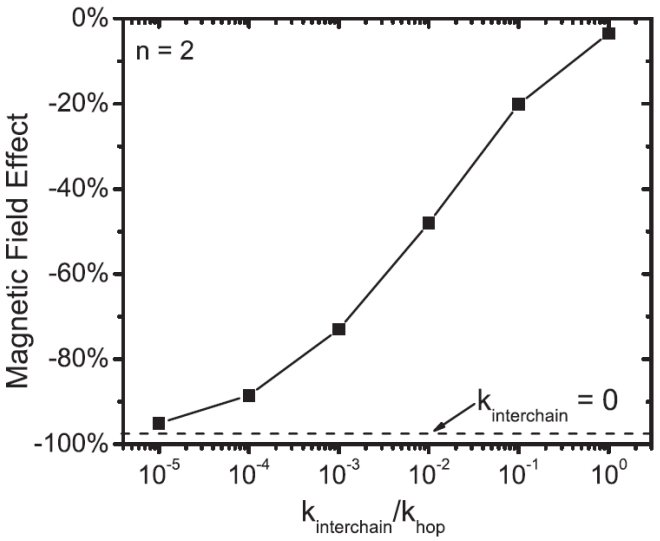

Figure 2: Relationship between magnetic field effect and ratio between interchain rate ($k_{interchain}$) and hopping rate (k_{hop}) in absence of disorder and at high electron density. Reproduced with permission from Ref[22]

precession rate; (ii) favouring 1D charge transport by reducing interchain hopping (Figure 2).

An interesting example of experimental engineering of the (radiative) charge traps within the active layer of the device and their role on OMAR was explored by Cox et al.[18] The authors conceived an experiment where the magnetic field effects measured in several co-polymers were also monitored by optical spectroscopy. The co-polymers were built by combining different polymer units, each one possessing distinct emission properties which allowed direct spectroscopic monitoring of the related magnetic phenomena. Their findings confirmed that spin mixing at the traps sites is responsible for the large OMAR effects observed experimentally.

Furthermore, the role of the dielectric/semiconductor and metal/semiconductor interfaces on OMAR is also rather unexplored. While organic semiconductors can be considered as *van der Waals* molecular solids, where the molecular interactions are rather weak, this character has strong repercussions on their structural and energetic order which is much lower compared to their inorganic counterparts. The dependence of charge transport and injection on the interfaces presents a challenge but can be turned into an advantage for tuning the OMAR effect. It is widely accepted that in organic field-effect transistors charges move near to the semiconductor/dielectric interface and hence control over possible structural and energetic disorder at the interface is of paramount importance[35]. For instance, it has been shown by several studies that high-k dielectrics influence the distribution of the DOS by creating dipolar disorder at the interface with the semiconductor[36, 37]. More precisely, the dipolar disorder generates a broadening of the DOS. The broadening is mostly due to energy fluctuations generated by local and randomly oriented dipoles. We believe this is an important parameter affecting the bipolaron formation since it is intimately related to the width of the DOS. When such width is large, charge carriers will experience a higher hopping barrier which will increase the magnetoresistance and lead to higher local concentrations of bipolarons with respect to the case where low-k dielectrics are used. Molecular engineering of the metal/semiconductor interface certainly represents a powerful tool to enhance OMAR. As an example, it has been widely reported in literature that various physical and chemical properties such as the metal work function can be adjusted by using various self-assembled monolayers (SAMs) chemisorbed on metal electrodes.[38, 39] Surface modifications of metal electrodes via SAMs are typically done to achieve energetic alignment between the metal work function, Φ_m, and the HOMO (LUMO) level of the organic semiconductor or at least to reduce the charge injection barrier at such interface. Interfacial morphology and tunnelling resistance associated to the SAM have also been found to strongly influence the charge injection as has been reported for alkanethiol-coated electrodes.[40] A recent study[20] reported on the effect of the insertion of a fluoro-SAM functionalized gold electrode on the associated magnetoresistance. Interestingly, the authors found that a central role was played by the change in interfacial morphology due to the change in wettability upon chemisorption of the SAM. Furthermore, insertion of the fluoro-SAM led to the intriguing discovery that the sign of the OMAR could change. Whilst this further underlines the significant impact of morphology and structural order of the semiconductor on the magnetoresistance, the effect of a strong interfacial molecular dipole (which led to an increase in the measured work-function) could not be disentangled from the morphological effects and this and other aspects will certainly need to be analysed more in depth in the near future.

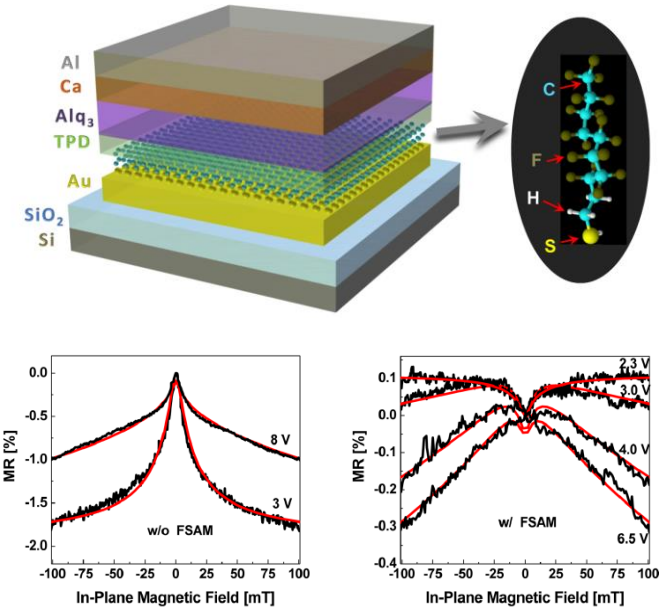

Figure 3: (Top panel) Schematic layout of the Au/TPD/Alq3/Ca device that includes a Au bottom electrode functionalised with fluorinated self-assembled monolayers (F-SAM). (Bottom panel) Magnetoresistance variation vs. in-plane magnetic field of the with (right) and without (left) F-SAM treatment on Au. The measurements were realized at room temperature with a bias voltage of 3.0 and 8.0 V (black lines).The data were fitted with a combined model of empirical non-Lorentzian and √B dependence (red lines).Reproduced with permission from Ref[20] Copyright

2. Organic thermoelectric materials

2.1 Overview of organic thermoelectrics

A thermoelectric device typically consists of two thermoelectric materials, one *p*-type and one *n*-type semiconductor, sandwiched between a hot electrode ($\boldsymbol{T} = \boldsymbol{T_h}$) and a cold one ($\boldsymbol{T} = \boldsymbol{T_c}$) as schematised in Figure 4a. Greater thermal motion of charge carriers at the hot side compared to the cold leads to a charge density

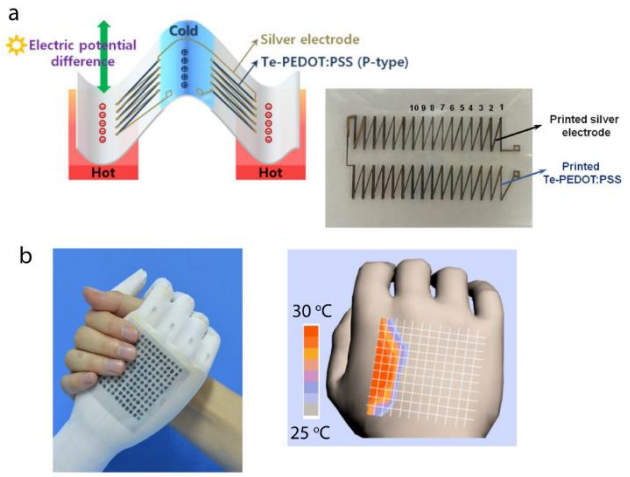

Figure 4: a Schematic of a planar printed thermoelectric device (left) incorporating a *p*-type hybrid polymer-inorganic material (Te-PEDOT:PSS). The n-type legs are substituted with silver. The printed device is shown on the right. Reproduced from Bae et al.[2] with permission….. b A wearable microstructure-frame-supported organic thermoelectric device able to detect temperature and pressure changes (left). Temperature map (right) detected from the same device. Reproduced from Zhang et al.[9]

gradient which opposes the temperature gradient. This can be detected as a thermal voltage, $\boldsymbol{\Delta V}$, across the two sides of the material whose magnitude is governed by the material's Seebeck coefficient, $\boldsymbol{S = \Delta V/\Delta T}$, and allows useful electrical power to be extracted.

The maximum efficiency, η_{TE}, of any thermoelectric device can be written as a function of the Carnot efficiency, $\boldsymbol{\eta_c = (T_h - T_c)/T_h}$.

$$\eta_{TE} = \eta_c \frac{\sqrt{1+zT}-1}{\sqrt{1+zT}+1-\eta_c} \qquad (3)$$

where $\boldsymbol{T = (T_h - T_c)/2}$. Here the dimensionless factor, *ZT*, known as the thermoelectric figure of merit, is the material parameter at temperature, T, that needs to be maximised and can be expanded as a function of the material's conductivity, σ, Seebeck coefficient, *S*, and thermal conductivity, κ.

$$\boldsymbol{ZT = \sigma S^2 T/\kappa} \qquad (4)$$

A good thermoelectric material must therefore possess a high electrical conductivity combined with a large Seebeck coefficient and a low thermal conductivity. ZT ≥ 1 is generally considered necessary for most applications. The great challenge of developing improved organic thermoelectric materials is the strong interdependence between the three thermoelectric properties σ, S and κ, with optimisation of any one property having a detrimental effect on at least one of the others. In what follows, some of the strategies material development are discussed. It should be noted that eq. 4 only holds for small ($\boldsymbol{T_h - T_c}$), i.e. small enough that S is constant over the range $\boldsymbol{T_c < T < T_h}$ and therefore that the Thomson effect is not significant, otherwise an integral form of eq. 3 should be adopted.[41]

Organic materials whose thermoelectric properties have been studied[42] include polymers such as poly(thienothiophene),[43] poly(ethylene-dioxythiophene)[44-50] (PEDOT), polyaniline,[51] poly(*p*-phenylene vinylene) derivatives,[52, 53] poly(3-hexylthiophene),[1, 54] carbazole polymers,[55-57] metal coordination polymers,[58] and P(NDIOD-T2)[59], as well as small molecules such as fullerenes,[60-63] perylene diimide derivatives and organic salts based on TTF, TCNQ, BEDT-TTF and tetrathiotetracene amongst others.[44, 64-70] Of these, PEDOT has recently shown excellent performance as a p-type thermoelectric material with *ZT* reported up to 0.42[71]. On the other hand, there has not been so much success in finding good n-type organic thermoelectric materials. Nonetheless *ZT* of up to 0.3 has been observed for poly(metal 1,1,2,2-ethenetetrathiolates)[58, 72] with reasonable power factors (σS^2) of >400 μWm^{-1} K^{-2}.[72]

2.2 Doping of organic thermoelectric materials

The conductivity of a material, *σ*, is proportional to the charge carrier mobility in that material, *μ*, and the carrier concentration, *N*:

$$\sigma = eN\mu \qquad (5)$$

Thermoelectric materials are therefore metals or doped semiconductors and for most organic thermoelectric materials this means combining a high mobility intrinsic organic semiconductor with a suitable dopant, though there are also a few examples of organic thermoelectric materials which derive their conductivity through self-doping.[58, 73, 74] Doped polymer films can be produced with conductivities >3000 S cm^{-1}.[75]

Choosing a suitable dopant requires consideration of its oxidation or reduction potential relative to the transport level of the semiconductor, the doping efficiency in the target semiconductor and the degree of doping required. Atomic and small molecule dopants such as lithium, strontium, iodine, bromine or certain Lewis acids are sometimes used[53, 76-79] but are often not ideal for devices as they can diffuse at moderate temperatures and reduce operating lifetimes.[80] Molecular dopants are usually preferable as they are less mobile in the solid state.

P-type molecular dopants include 7,7,8,8-tetracyanoquinodimethane (TCNQ), 2,3,5,6-tetrafluoro-7,7,8,8-tetracyanoquinodimethane (F_4-TCNQ),[81] tosylate (Tos),[44, 50] poly(styrenesulfonate)[2, 49] (PSS) and chloranil[82] amongst others. Since an n-type molecular dopant must possess a HOMO above the LUMO of the semiconductor they are typically less chemically stable and the options are much reduced. Examples are dihydro-1H-benzoimidazol-2-yl (N-DBI),[59] bis(ethylenedithio)-tetrathiafulvalene (BEDT-TTF),[83] tetrathianaphthacene (TTN),[84] bis(cyclopentadienyl)-cobalt(II) (cobaltocene, CoCp2)[85] and dimetal complexes.[61, 86, 87] Alkali metals may also be used, but with the limitations on device lifetime noted above. A way around chemical or device stability

issues is to use air-stable dopant precursors that dope through an intermediate state as is the case for rhodocene dimers[88] and some cationic dyes.[89, 90]

Since increasing the conductivity can decrease the Seebeck coefficient and increase the thermal conductivity (vide infra), optimum doping levels for thermoelectric applications are typically a little lower than for solely high conductivity applications. In the case of PEDOT: PSS or PEDOT:Tos, for example, acido-basic control of conductivity[2, 50] can be achieved by immersion of the pre-deposited films in acidic or basic solutions can be used to de-dope the as-synthesised material to maximise *ZT*. A number of post-deposition solvent treatments are also available which can boost conductivity and *ZT* such as rinsing with (di)ethylene glycol, DMF, H_2SO_4 or DMSO.[2, 49, 71, 91]

Typical charge carrier concentrations in optimised thermoelectric mateirals are ~10^{18}-10^{20} /cm^3.[2, 46] Introducing the required quantity of dopants will have an impact on the packing and geometry of the semiconductor. Furthermore, the dopants increase ionised impurity scattering[46] and can cause a broadening of the density of states in the semiconductor.[81] It is therefore a complex challenge to increase *N* without reducing μ. Nonetheless, this is possible in PEDOT due to the aromatic to quinoid transition at high doping levels. The quinoid form is more planar which allows a higher degree of crystallinity and shorter π-stacking distances[46, 91] but for many materials μ decreases with increasing doping.

It is important to ensure a high doping efficiency to reduce number of dopants to achieve the desired *N*. This is determined partly by oxidation/reduction potentials of the dopant relative to the transport level of the semiconductor, but also by the geometrical configuration of the dopant-semiconductor system.[92] In certain donor-acceptor copolymers, the p-dopant F_4-TCNQ located in the vicinity of the acceptor units contribute little to charge transfer compared to when it is located over acceptor units.[93, 94] Further factors which may limit the doping efficiency include phase segregation of the dopants,[59, 94] the degree of delocalisation of the dopant-induced charge on the molecule/polymer[93] and changes to the energy landscape caused either by frontier orbital hybridisation between the dopant and semiconductor[46] or by ion-induced density of states broadening.[81] To take an example, charge transfer between F_4-TCNQ and P3HT is very efficient (up to 100%).[81] However, the associated free charge density is very low, perhaps just 5% of the dopant density, with the remaining charges being Coulombically bound to the F_4-TCNQ anion. Much higher (free charge) doping efficiencies (~90%) are observed for PEDOT:Tos.[46]

An alternative approach to study molecular thermoelectric materials under high levels of doping is to use organic field effect transistors[54] (OFETs) or electrochemically gated organic field-effect transistors[47, 54] (EG-OFET). This approach has the advantages of controlled gate modulation of the charge carrier density over orders of magnitude and the possibility of high doping levels (nearly 50% of the monomer density for EG-OFETS[47]) without altering the film morphology, though it is not a suitable architecture for a thermoelectric generator. In fact, with this approach, large power factors (σS^2) are reported for the polymers PBTTT and P3HT[54] that match or exceed those obtained for PEDOT EG-OFETs[47]. This result strongly suggests that accurate control morphology whilst doping may open up the range of organic thermoelectric materials exhibiting ZT > 0.1.

2.3 Molecular control over the Seebeck coefficient

Engineering of the Seebeck coefficient, *S*, in organic thermoelectric materials has not been so extensively explored. Here we will highlight some key relations and discuss how these relate to *S* in organic materials. For intrinsic semiconductors, *S* is linked to the difference in energy between the Fermi level, E_F, and the transport level, E_{trans}, by the Boltzman equation:

$$S = \frac{k_B}{e}\left[\left(\frac{E_F - E_{trans}}{k_B T}\right) - A\right] \quad (6)$$

where A is the heat of transport.[80] This equation is written for one charge carrier type only since minority charge carriers will reduce *S*.[51] There are important approximations in the derivation of the Boltzman equation, including the assumption of discrete energy levels rather than the Gaussian broadened levels generally assumed for organic semiconductors.[80] Nonetheless, one immediately visible consequence of eq. 6 is that doping an organic semiconductor, which is necessary for high conductivity will reduce the Seebeck coefficient by moving the Fermi level, E_F, closer to the transport level, E_{trans}.

For heavily doped systems, where $\boldsymbol{E_F \approx E_{trans}}$, *A* can become significant. This is the case for many organic thermoelectric materials, including PEDOT which can be considered a semi-metal under certain conditions.[91] In this regime, the Boltzman equation reduces to the Mott relationship[95, 96]:

$$S \approx \mathrm{A} \approx \frac{\pi^2 {k_B}^2 T}{3e}\left(\frac{d(\ln \sigma)}{dE}\right)_{E_F} = \frac{\pi^2 {k_B}^2 T}{3e}\left(\frac{1}{N}\cdot\frac{d\mathrm{N(E)}}{d\mathrm{E}} + \frac{1}{\mu}\cdot\frac{d\mu(\mathrm{E})}{d\mathrm{E}}\right)_{E_F} \quad (7)$$

Importantly it can be seen that *S* is maximised by a sharp increase in the density of states around the Fermi level. For metals as well as highly oxidized polyaniline[51] the Fermi level lies in the middle of the band and they therefore have low thermopower. An $\boldsymbol{S \propto \ln \sigma}$ relationship is commonly observed for polymers including polyaniline,[51] and P3HT[1] (Figure 5a).

Improved order in a polymer film is one way to boost σ without decreasing *S*. For example, the $\mathbf{S \propto \ln \sigma}$ relationship is maintained in polyaniline films upon doping, yet stretching the films to align the polymer can boost σ at a fixed *S*.[51] This emerges from a reduction in localised energy levels near E_F that tend to smooth out the density of states. A similar effect can also be achieved in PEDOT by using a number of solvent additives which improve ordering in resultant films.[91] Counterintuitively, the Seebeck coefficient in PEDOT:ToS films has been shown to increase with conductivity. This remarkable result is attributed to its bipolaronic band structure with an empty bipolaron band merging into the valence band. This semi-metallic

electronic structure possesses a rapidly varying density of states at the Fermi level which is highly sensitive to structural order and allows the increase of Seebeck coefficient with increasing conductivity.

2.4 Controlling thermal conductivity

Inorganic thermoelectric materials suffer in most cases from high thermal conductivity which often has to be reduced by nanostructuring to introduce interfaces (grain boundaries or inclusions) which scatter phonons more strongly than electrons.[97, 98] Intrinsic organic semiconductors exhibit low thermal conductivities of $\kappa \approx 0.1 - 1$ *W/mK* [44, 99] which are equal to or lower than most state-of-the-art nanostructured inorganic materials. Due to this intrinsically low thermal conductivity, efforts to engineer high *ZT* organic materials have mostly focussed on improving σ and *S*. Nonetheless, κ remains important and a deeper understanding is required to establish whether organic thermoelectric materials can achieve, for example, the ultra-low thermal conductivities of certain fullerenes such as PCBM (0.03-0.05 W/mK[100-102]).

Thermal conductivity, $\boldsymbol{\kappa}$ comprises lattice and eletronic contributions, $\boldsymbol{\kappa_L}$ and $\boldsymbol{\kappa_E}$ respectively, where $\boldsymbol{\kappa = \kappa_L + \kappa_E}$. The electronic component is intimately linked to the electrical conductivity, σ, by the Wiedemann-Franz Law, $\boldsymbol{\kappa_E = \sigma LT}$, where *L* is the Lorentz number. Therefore, reducing thermal conductivity in thermoelectric materials must focus on minimising $\boldsymbol{\kappa_L}$ and the Lorentz number, *L*. The value of $\boldsymbol{\kappa_L}$ is linked to phonon scattering and is decreased by grain boundaries and disorder, by designing molecules whose composite atoms span a wide range of atomic weights, or by including loosely bound atoms in the structure (so-called rattling modes). An example of the latter are the poly(metal 1,1,2,2-ethenetetrathiolate)s[58] which exhibit a modest thermal conductivity over a wide temperature range.

L has been measured for PEDOT:PSS[3, 103] and PEDOT:Tos.[103]. The validity of the Wiedemann-Franz law was verified, but there is still debate over the value of *L*, with two reports[3, 104] suggesting *L* is equal to the Sommerfeld value for a free electron gas, $L_s = 2.45 \times 10^{-8}$ *WΩK*$^{-2}$,[105] and another two[103, 106] differing values of *L*. On top of this, theoretical work further suggests $L < L_s$ for low/intermediate doping concentrations in PEDOT:Tos.[46] Charge transport in organic materials involves polarons and in polymers involves quasi-1-dimensional along-chain transport[103] and therefore it should not be assumed that the Sommerfeld value must apply. The impact of the value of *L* on *ZT* is significant: $\boldsymbol{\kappa}$ increases by a factor of up to 3 between intrinsic PEDOT and PEDOT doped to levels typical for thermoelectric applications.[3, 103] How one might engineer *L* by molecular design is not yet clear, but perhaps some lessons should be learned from the inorganic community where it is known that the Lorenz number can be decreased by reducing the bandwidth of the charge carrier dispersion[107] and can be tuned by nanostructuring.[108, 109]

3. Outlook

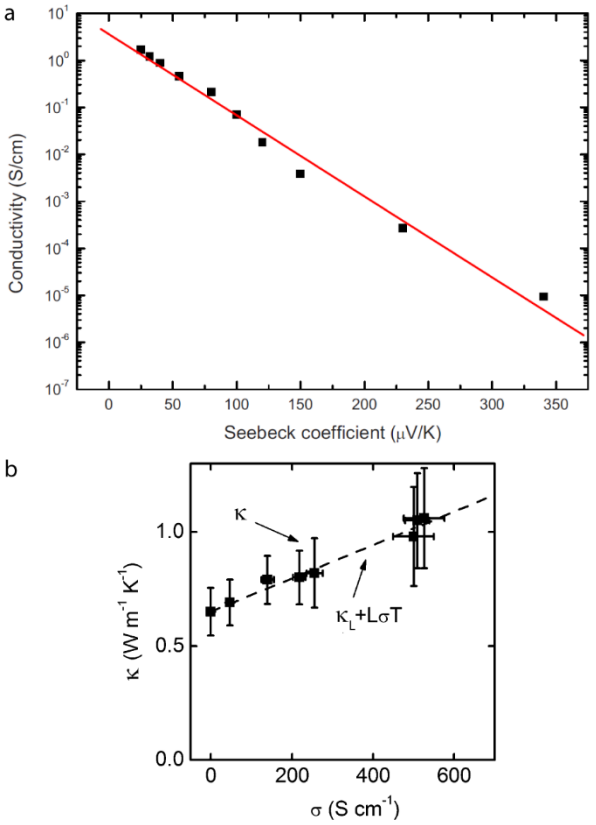

Figure 5: a Conductivty plotted against Seebeck coefficient for P3HT films, showing the typical $S \propto \ln \sigma$ relationship. Reproduced from Xuan et al.[1] with permission..... **b** In-plane thermal conductivity plotted against electrical conductivity for DMSO-mixed PEDOT:PSS. Adapted from Liu et al.[3] with permission

Organic thermoelectric materials have been incorporated into flexible prototype devices either as conventional or planar thermoelectric generators[2] or as thermal sensors.[9] However, improvements in materials design are still needed to boost output powers and efficiencies of thermoelectric generators. There are a number of organic materials with charge carrier mobilities greater than PEDOT[110-115] which gives us hope that the necessary improvements in *ZT* are within reach. This is especially true for n-type organic materials which are currently under-performing in thermoelectrics, which places limits on the performance of all-organic thermoelectric generators. By combining improved materials with improved processing focussing on molecular (polymer) alignment[51, 116], morphology and hybrid composites[2, 45, 117] there is a great potential for efficient organic thermoelectric generators in the near future.

Analogously, a rigorous material design is needed for controlling spin mixing rules and therefore achieving control over magnetoresistance. In this regard, 1D wires minimizing the *inter*chain hopping would be the most suitable structure to achieve such goal. This represents an important design rule for the materials which would be counterintuitive for attaining good charge transport. It is important that synthetic chemists in these fields focus on new design rules specific to magnetoresistance and thermoelectricity rather than on legacy design rules for charge transport materials.

Furthermore, a number of doping strategies are yet be explored for controlling the thermoelectric and magnetoresistive properties of the films. The doping can be either substitutional (addition of molecular units to a given polymer chain/molecule) or interstitial (by blending with a second material).

In conclusion, the research fields of organic magnetoresistance and thermoelectrics are relatively fresh but there is already a body of research which is beginning to unravel the underlying mechanisms in these materials. This work emphasizes the fact that a concerted synthetic effort is needed to develop a new generation of materials with a more tailored molecular design.

Acknowledgements

OF is a Royal Society University Research Fellow. EO thanks Dr. M. Gobbi and Prof. L.H. Hueso for fruitful discussions.

Notes and references

1. Y. Xuan, X. Liu, S. Desbief, P. Leclère, M. Fahlman, R. Lazzaroni, M. Berggren, J. Cornil, D. Emin and X. Crispin, *Phys. Rev. B*, 2010, **82**, 115454.
2. E. Jin Bae, Y. Hun Kang, K.-S. Jang and S. Yun Cho, *Sci. Rep.*, 2016, **6**, 18805.
3. J. Liu, X. J. Wang, D. Y. Li, N. E. Coates, R. A. Segalman and D. G. Cahill, *Macromolecules*, 2015, **48**, 585-591.
4. V. A. Dediu, L. E. Hueso, I. Bergenti and C. Taliani, *Nature Mater.*, 2009, **8**, 707 - 716.
5. O. Mermer, G. Veeraraghavan, T. L. Francis, Y. Sheng, D. T. Nguyen, M. Wohlgenannt, A. Kohler, M. K. Al-Suti and M. S. Khan, *Phys. Rev. B*, 2005, **72**, 205202.
6. B. Hu, L. A. Yan and M. Shao, *Adv. Mater.*, 2009, **21**, 1500-1516.
7. P. A. Bobbert, T. D. Nguyen, F. W. A. van Oost, B. Koopmans and M. Wohlgenannt, *Phys. Rev. Lett.*, 2007, **99**, 216801.
8. V. N. Prigodin, J. D. Bergeson, D. M. Lincoln and A. J. Epstein, *Synth. Met.*, 2006, **156**, 757-761.
9. F. Zhang, Y. Zang, D. Huang, C.-a. Di and D. Zhu, *Nat Commun*, 2015, **6**.
10. T. L. Francis, O. Mermer, G. Veeraraghavan and M. Wohlgenannt, *New J. Phys.*, 2004, **6**.
11. S. A. Bagnich, U. Niedermeier, C. Melzer, W. Sarfert and H. von Seggern, *J. Appl. Phys.*, 2009, **105**, 123706.
12. F. L. Bloom, M. Kemerink, W. Wagemans and B. Koopmans, *Phys. Rev. Lett.*, 2009, **103**, 066601.
13. J. D. Bergeson, V. N. Prigodin, D. M. Lincoln and A. J. Epstein, *Phys. Rev. Lett.*, 2008, **100**, 067201.
14. F. L. Bloom, W. Wagemans and B. Koopmans, *J. Appl. Phys.*, 2008, **103**, 07F320.
15. P. A. Bobbert, W. Wagemans, F. W. A. van Oost, B. Koopmans and M. Wohlgenannt, *Phys. Rev. Lett.*, 2009, **102**, 156604.
16. M. Cox, P. Janssen, F. Zhu and B. Koopmans, *Phys. Rev. B*, 2013, **88**, 035202.
17. M. Cox, E. H. M. van der Heijden, P. Janssen and B. Koopmans, *Phys. Rev. B*, 2014, **89**, 085201.
18. M. Cox, M. H. A. Wijnen, G. A. H. Wetzelaer, M. Kemerink, P. W. M. Blom and B. Koopmans, *Phys. Rev. B*, 2014, **90**, 155205.
19. J. Danon, X. H. Wang and A. Manchon, *Phys. Rev. Lett.*, 2013, **111**, 066802.
20. H. J. Jang, S. J. Pookpanratana, A. N. Brigeman, R. J. Kline, J. I. Basham, D. J. Gundlach, C. A. Hacker, O. A. Kirillov, O. D. Jurchescu and C. A. Richter, *ACS Nano*, 2014, **8**, 7192-7201.
21. P. Janssen, M. Cox, S. H. W. Wouters, M. Kemerink, M. M. Wienk and B. Koopmans, *Nature Comm.*, 2013, **4**, 2286.
22. S. P. Kersten, S. C. J. Meskers and P. A. Bobbert, *Phys. Rev. B* 2012, 045210.
23. R. N. Mahato, H. Lulf, M. H. Siekman, S. P. Kersten, P. A. Bobbert, M. P. de Jong, L. De Cola and W. G. van der Wiel, *Science*, 2013, **341**, 257-260.
24. U. Niedermeier, M. Vieth, R. Patzold, W. Sarfert and H. von Seggern, *Appl. Phys. Lett.*, 2008, **92**, 193309.
25. J. Rybicki, R. Lin, F. Wang, M. Wohlgenannt, C. He, T. Sanders and Y. Suzuki, *Phys. Rev. Lett.*, 2012, **109**, 076603.
26. A. J. Schellekens, W. Wagemans, S. P. Kersten, P. A. Bobbert and B. Koopmans, *Phys. Rev. B*, 2011, **84**, 075204.
27. Y. Sheng, T. D. Nguyen, G. Veeraraghavan, O. Mermer, M. Wohlgenannt, S. Qiu and U. Scherf, *Phys. Rev. B*, 2006, **74**, 045213.
28. M. Wohlgenannt, P. A. Bobbert and B. Koopmans, *Mrs Bulletin*, 2014, **39**, 590-595.
29. S. Zanettini, G. Chaumy, P. Chavez, N. Leclerc, C. Etrillard, B. Leconte, F. Chevrier, J. F. Dayen and B. Doudin, *J Phys-Condens Mat*, 2015, **27**, 462001.
30. S. Zanettini, J. F. Dayen, C. Etrillard, N. Leclerc, M. V. Kamalakar and B. Doudin, *Appl. Phys. Lett.*, 2015, **106**, 063303.
31. M. N. Bussac and L. Zuppiroli, *Phys. Rev. B*, 1993, **47**, 5493.
32. A. Salleo and R. A. Street, *Phys. Rev. B*, 2004, **70**, 235324.
33. R. A. Street, A. Salleo and M. L. Chabinyc, *Phys. Rev. B*, 2003, **68**, 085316.
34. X. M. Jiang, R. Österbacka, O. Korovyanko, C. P. An, B. Horovitz, R. A. J. Janssen and Z. V. Vardeny, *Adv. Funct. Mater.*, 2002, **12**, 587–597.
35. F. Dinelli, M. Murgia, P. Levy, M. Cavallini, F. Biscarini and D. M. de Leeuw, *Phys. Rev. Lett.*, 2004, **92**, 116802.
36. J. Veres, S. D. Ogier, S. W. Leeming, D. C. Cupertino and S. M. Khaffaf, *Adv. Funct. Mater.*, 2003, **13**, 199-204.
37. I. N. Hulea, S. Fratini, H. Xie, C. L. Mulder, N. N. Iossad, G. Rastelli, S. Ciuchi and A. F. Morpurgo, *Nature Mater.*, 2006, **5**, 982-986.
38. I. H. Campbell, S. Rubin, T. A. Zawodzinski, J. D. Kress, R. L. Martin, D. L. Smith, N. N. Barashkov and J. P. Ferraris, *Phys. Rev. B*, 1996, **54**, 14321-14324.
39. B. de Boer, A. Hadipour, M. M. Mandoc, T. van Woudenbergh and P. W. M. Blom, *Adv. Mater.*, 2005, **17**, 621-625.
40. P. Stoliar, R. Kshirsagar, M. Massi, P. Annibale, C. Albonetti, D. M. de Leeuw and F. Biscarini, *J. Am. Chem. Soc.*, 2007, **129**, 6477-6484.
41. H. S. Kim, W. Liu, G. Chen, C.-W. Chu and Z. Ren, *Proc. Natl. Acad. Sci.* , 2015, **112**, 8205-8210.
42. P. J. Taroni, I. Hoces, N. Stingelin, M. Heeney and E. Bilotti, *Isr. J. Chem.*, 2014, **54**, 534-552.
43. R. Yue, S. Chen, B. Lu, C. Liu and J. Xu, *J Solid State Electrochem*, 2011, **15**, 539-548.

44. O. Bubnova, Z. U. Khan, A. Malti, S. Braun, M. Fahlman, M. Berggren and X. Crispin, *Nature Mater.*, 2011, **10**, 429-433.
45. K. Wei, T. Stedman, Z. H. Ge, L. M. Woods and G. S. Nolas, *Appl. Phys. Lett.*, 2015, **107**, 153301.
46. W. Shi, T. Zhao, J. Xi, D. Wang and Z. Shuai, *J. Am. Chem. Soc.*, 2015, **137**, 12929-12938.
47. O. Bubnova, M. Berggren and X. Crispin, *J. Am. Chem. Soc.*, 2012, **134**, 16456-16459.
48. C. Liu, B. Lu, J. Yan, J. Xu, R. Yue, Z. Zhu, S. Zhou, X. Hu, Z. Zhang and P. Chen, *Synth. Met.*, 2010, **160**, 2481-2485.
49. E. Liu, C. Liu, Z. Zhu, H. Shi, Q. Jiang, F. Jiang, J. Xu, J. Xiong and Y. Hu, *J. Polym. Res.*, 2015, **22**, 1-5.
50. Z. U. Khan, O. Bubnova, M. J. Jafari, R. Brooke, X. Liu, R. Gabrielsson, T. Ederth, D. R. Evans, J. W. Andreasen, M. Fahlman and X. Crispin, *J. Mater. Chem. C*, 2015, **3**, 10616-10623.
51. N. Mateeva, H. Niculescu, J. Schlenoff and L. R. Testardi, *J. Appl. Phys.*, 1998, **83**, 3111-3117.
52. Y. Hiroshige, M. Ookawa and N. Toshima, *Synth. Met.*, 2007, **157**, 467-474.
53. Y. Hiroshige, M. Ookawa and N. Toshima, *Synth. Met.*, 2006, **156**, 1341-1347.
54. F. Zhang, Y. Zang, D. Huang, C.-a. Di, X. Gao, H. Sirringhaus and D. Zhu, *Adv. Funct. Mater.*, 2015, **25**, 3004-3012.
55. R. B. Aïch, N. Blouin, A. Bouchard and M. Leclerc, *Chem. Mat.*, 2009, **21**, 751-757.
56. I. Lévesque, P.-O. Bertrand, N. Blouin, M. Leclerc, S. Zecchin, G. Zotti, C. I. Ratcliffe, D. D. Klug, X. Gao, F. Gao and J. S. Tse, *Chem. Mat.*, 2007, **19**, 2128-2138.
57. I. Lévesque, X. Gao, D. D. Klug, J. S. Tse, C. I. Ratcliffe and M. Leclerc, *React. Funct. Polym.*, 2005, **65**, 23-36.
58. Y. Sun, P. Sheng, C. Di, F. Jiao, W. Xu, D. Qiu and D. Zhu, *Adv. Mater.*, 2012, **24**, 932-937.
59. R. A. Schlitz, F. G. Brunetti, A. M. Glaudell, P. L. Miller, M. A. Brady, C. J. Takacs, C. J. Hawker and M. L. Chabinyc, *Adv. Mater.*, 2014, **26**, 2825-2830.
60. Z. H. Wang, K. Ichimura, M. S. Dresselhaus, G. Dresselhaus, W. T. Lee, K. A. Wang and P. C. Eklund, *Phys. Rev. B*, 1993, **48**, 10657-10660.
61. T. Menke, D. Ray, J. Meiss, K. Leo and M. Riede, *Appl. Phys. Lett.*, 2012, **100**, 093304.
62. M. Sumino, K. Harada, M. Ikeda, S. Tanaka, K. Miyazaki and C. Adachi, *Appl. Phys. Lett.*, 2011, **99**, 093308.
63. L. Rincon-Garcia, A. K. Ismael, C. Evangeli, I. Grace, G. Rubio-Bollinger, K. Porfyrakis, N. Agrait and C. J. Lambert, *Nature Mater.*, 2016, **15**, 289-293.
64. W. Jens and P.-K. Karin, *J. Phys. D-Appl. Phys.*, 2008, **41**, 135113.
65. E. A. Perez-Albuerne, H. Johnson and D. J. Trevoy, *J. Chem. Phys.*, 1971, **55**, 1547-1554.
66. J. W. Bray, H. R. Hart, L. V. Interrante, I. S. Jacobs, J. S. Kasper, P. A. Piacente and G. D. Watkins, *Phys. Rev. B*, 1977, **16**, 1359-1364.
67. M. G. Miles and J. D. Wilson, *Inorg. Chem.*, 1975, **14**, 2357-2360.
68. A. Casian and I. Sanduleac, *Journal of Elec Materi*, 2014, **43**, 3740-3745.
69. L. C. Isett, *Phys. Rev. B*, 1978, **18**, 439-447.
70. A. Casian and I. Sanduleac, *Mater. Today: Proceedings*, 2015, **2**, 504-509.
71. G. H. Kim, L. Shao, K. Zhang and K. P. Pipe, *Nature Mater.*, 2013, **12**, 719-723.
72. Y. Sun, L. Qiu, L. Tang, H. Geng, H. Wang, F. Zhang, D. Huang, W. Xu, P. Yue, Y.-s. Guan, F. Jiao, Y. Sun, D. Tang, C.-a. Di, Y. Yi and D. Zhu, *Advanced Materials*, 2016, **28**, 3351-3358.
73. B. Russ, M. J. Robb, F. G. Brunetti, P. L. Miller, E. E. Perry, S. N. Patel, V. Ho, W. B. Chang, J. J. Urban, M. L. Chabinyc, C. J. Hawker and R. A. Segalman, *Adv. Mater.*, 2014, **26**, 3473-3477.
74. C.-K. Mai, R. A. Schlitz, G. M. Su, D. Spitzer, X. Wang, S. L. Fronk, D. G. Cahill, M. L. Chabinyc and G. C. Bazan, *J. Am. Chem. Soc.*, 2014, **136**, 13478-13481.
75. M. V. Fabretto, D. R. Evans, M. Mueller, K. Zuber, P. Hojati-Talemi, R. D. Short, G. G. Wallace and P. J. Murphy, *Chem. Mat.*, 2012, **24**, 3998-4003.
76. J. Puigmartí-Luis, V. Laukhin, Á. Pérez del Pino, J. Vidal-Gancedo, C. Rovira, E. Laukhina and D. B. Amabilino, *Angew. Chem. Int. Ed.*, 2007, **46**, 238-241.
77. G. Parthasarathy, C. Shen, A. Kahn and S. R. Forrest, *J. Appl. Phys.*, 2001, **89**, 4986-4992.
78. J. Kido and T. Matsumoto, *Appl. Phys. Lett.*, 1998, **73**, 2866-2868.
79. E. Jun, M. Toshio and K. Junji, *Jpn. J. Appl. Phys.*, 2002, **41**, L358.
80. B. Lüssem, M. Riede and K. Leo, *Phys. Status Solidi A-Appl. Mat.*, 2013, **210**, 9-43.
81. P. Pingel and D. Neher, *Phys. Rev. B*, 2013, **87**, 115209.
82. D. R. Kearns, G. Tollin and M. Calvin, *J. Chem. Phys.*, 1960, **32**, 1020-1025.
83. A. Nollau, M. Pfeiffer, T. Fritz and K. Leo, *J. Appl. Phys.*, 2000, **87**, 4340-4343.
84. T. Senku, K. Kaname, K. Eiji, I. Takashi, N. Toshio, O. Yukio and S. Kazuhiko, *Jpn. J. Appl. Phys.*, 2005, **44**, 3760.
85. C. K. Chan, F. Amy, Q. Zhang, S. Barlow, S. Marder and A. Kahn, *Chem. Phys. Lett.* , 2006, **431**, 67-71.
86. F. A. Cotton, N. E. Gruhn, J. Gu, P. Huang, D. L. Lichtenberger, C. A. Murillo, L. O. Van Dorn and C. C. Wilkinson, *Science*, 2002, **298**, 1971-1974.
87. F. A. Cotton, J. P. Donahue, D. L. Lichtenberger, C. A. Murillo and D. Villagrán, *J. Am. Chem. Soc.*, 2005, **127**, 10808-10809.
88. S. Guo, S. B. Kim, S. K. Mohapatra, Y. Qi, T. Sajoto, A. Kahn, S. R. Marder and S. Barlow, *Adv. Mater.*, 2012, **24**, 699-703.
89. A. Werner, F. Li, K. Harada, M. Pfeiffer, T. Fritz, K. Leo and S. Machill, *Adv. Funct. Mater.*, 2004, **14**, 255-260.
90. F. Li, A. Werner, M. Pfeiffer, K. Leo and X. Liu, *J. Phys. Chem. B*, 2004, **108**, 17076-17082.
91. O. Bubnova, Z. U. Khan, H. Wang, S. Braun, D. R. Evans, M. Fabretto, P. Hojati-Talemi, D. Dagnelund, J.-B. Arlin, Y. H. Geerts, S. Desbief, D. W. Breiby, J. W. Andreasen, R. Lazzaroni, W. M. Chen, I. Zozoulenko, M. Fahlman, P. J. Murphy, M. Berggren and X. Crispin, *Nature Mater.*, 2014, **13**, 190-194.
92. L. Zhu, E.-G. Kim, Y. Yi and J.-L. Brédas, *Chem. Mat.*, 2011, **23**, 5149-5159.
93. D. Di Nuzzo, C. Fontanesi, R. Jones, S. Allard, I. Dumsch, U. Scherf, E. von Hauff, S. Schumacher and E. Da Como, *Nat Commun*, 2015, **6**, 1-8.
94. K.-H. Yim, G. L. Whiting, C. E. Murphy, J. J. M. Halls, J. H. Burroughes, R. H. Friend and J.-S. Kim, *Adv. Mater.*, 2008, **20**, 3319-3324.
95. T. O. Poehler and H. E. Katz, *Energy Environ. Sci.*, 2012, **5**, 8110-8115.

96. M. Cutler and N. F. Mott, *Phys. Rev.*, 1969, **181**, 1336-1340.
97. M. S. Dresselhaus, G. Chen, M. Y. Tang, R. G. Yang, H. Lee, D. Z. Wang, Z. F. Ren, J. P. Fleurial and P. Gogna, *Adv. Mater.*, 2007, **19**, 1043-1053.
98. G. Chen, *Phys. Rev. B*, 1998, **57**, 14958-14973.
99. J. C. Duda, P. E. Hopkins, Y. Shen and M. C. Gupta, *Appl. Phys. Lett.*, 2013, **102**, 251912.
100. L. Chen, X. Wang and S. Kumar, *Sci. Rep.*, 2015, **5**, 12763.
101. X. Wang, C. D. Liman, N. D. Treat, M. L. Chabinyc and D. G. Cahill, *Phys. Rev. B*, 2013, **88**, 075310.
102. J. C. Duda, P. E. Hopkins, Y. Shen and M. C. Gupta, *Phys. Rev. Lett.*, 2013, **110**, 015902.
103. A. Weathers, Z. U. Khan, R. Brooke, D. Evans, M. T. Pettes, J. W. Andreasen, X. Crispin and L. Shi, *Adv. Mater.*, 2015, **27**, 2101-2106.
104. M. B. Salamon, J. W. Bray, G. Depasquale, R. A. Craven, G. Stucky and A. Schultz, *Phys. Rev. B*, 1975, **11**, 619-622.
105. C. Kittel, *Introduction to solid state physics*, Wiley, New York, 7th edn., 1996.
106. N. Mermilliod, L. Zuppiroli and B. Francois, *J. Phys.*, 1980, **41**, 1453-1458.
107. C. Jeong, R. Kim and M. S. Lundstrom, *J. Appl. Phys.*, 2012, **111**, 113707.
108. F. Völklein, H. Reith, T. W. Cornelius, M. Rauber and R. Neumann, *Nanotechnology*, 2009, **20**, 325706.
109. X. Zhang, Q.-G. Zhang, B.-Y. Cao, M. Fujii, K. Takahashi and T. Ikuta, *Chin. Phys. Lett.*, 2006, **23**, 936-938.
110. I. Kang, H.-J. Yun, D. S. Chung, S.-K. Kwon and Y.-H. Kim, *J. Am. Chem. Soc.*, 2013, **135**, 14896-14899.
111. R. Noriega, J. Rivnay, K. Vandewal, F. P. V. Koch, N. Stingelin, P. Smith, M. F. Toney and A. Salleo, *Nature Mater.*, 2013, **12**, 1038-1044.
112. G. Kim, S.-J. Kang, G. K. Dutta, Y.-K. Han, T. J. Shin, Y.-Y. Noh and C. Yang, *J. Am. Chem. Soc.*, 2014, **136**, 9477-9483.
113. H.-R. Tseng, H. Phan, C. Luo, M. Wang, L. A. Perez, S. N. Patel, L. Ying, E. J. Kramer, T.-Q. Nguyen, G. C. Bazan and A. J. Heeger, *Adv. Mater.*, 2014, **26**, 2993-2998.
114. D. Venkateshvaran, M. Nikolka, A. Sadhanala, V. Lemaur, M. Zelazny, M. Kepa, M. Hurhangee, A. J. Kronemeijer, V. Pecunia, I. Nasrallah, I. Romanov, K. Broch, I. McCulloch, D. Emin, Y. Olivier, J. Cornil, D. Beljonne and H. Sirringhaus, *Nature*, 2014, **515**, 384-388.
115. C. Luo, A. K. K. Kyaw, L. A. Perez, S. Patel, M. Wang, B. Grimm, G. C. Bazan, E. J. Kramer and A. J. Heeger, *Nano Letters*, 2014, **14**, 2764-2771.
116. H. Yan, T. Ohta and N. Toshima, *Macromol. Mater. Eng.*, 2001, **286**, 139-142.
117. C. Bounioux, P. Diaz-Chao, M. Campoy-Quiles, M. S. Martin-Gonzalez, A. R. Goni, R. Yerushalmi-Rozen and C. Muller, *Energy Environ. Sci.*, 2013, **6**, 918-925.